

THE ANATOMY OF A LONG GAMMA-RAY BURST: A SIMPLE CLASSIFICATION SCHEME FOR THE EMISSION MECHANISM(S).

D. BÉGUÉ^{1,2,‡} AND J. MICHAEL BURGESS^{1,2,†}

Draft version May 24, 2022

ABSTRACT

Ultra-relativistic motion and efficient conversion of kinetic energy to radiation are required by gamma-ray burst (GRB) observations, yet they are difficult to simultaneously achieve. Three leading mechanisms have been proposed to explain the observed emission emanating from GRB outflows: radiation from either relativistic internal or external shocks, or thermal emission from a photosphere. Previous works were dedicated to independently treating these three mechanisms and arguing for a sole, unique origin of the prompt emission of gamma-ray bursts. In contrast, herein, we first explain why all three models are valid mechanisms and that a contribution from each of them is expected in the prompt phase. Additionally, we show that a single parameter, the dimensionless entropy of the GRB outflow, determines which mechanism contributes the most to the emission. More specifically, internal shocks dominate for low values of the dimensionless entropy, external shocks for intermediate values and finally, photospheric emission for large values. We present a unified framework for the emission mechanisms of GRBs with easily testable predictions for each process.

1. INTRODUCTION

Gamma-ray bursts (GRBs) are the most luminous sources in the Universe, and yet, their emission mechanism(s) is still lacking a unique explanation, for reviews see Mészáros (2006); Pe’er (2015); Kumar & Zhang (2015). Observations of rapid temporal variability and extremely high-energy photons require GRBs to have ultra-relativistic motion of their outflow plasma with Lorentz factors at least as high as a few hundred (Piran & Shemi 1993), implying that most of the energy of the burst is in kinetic form. Such large Lorentz factor are also indirectly suggested by the non-observation of neutrinos in coincidence with GRBs (Abbasi et al. 2012) and the constraints from the early optical afterglow, see *e.g.* Rykoff et al. (2009).

Therefore, efficient conversion of kinetic energy to radiation is required for any model attempting to explain the extreme isotropic⁵ luminosities ($\gtrsim 10^{51}$ erg s⁻¹) produced in GRBs. The leading mechanisms are the internal shock model (Rees & Mészáros 1994; Daigne & Mochkovitch 1998) (hereafter IS), the external shock model (Mészáros & Rees 1993; Chiang & Dermer 1999) (hereafter ES), and photospheric models (Goodman 1986; Paczyński 1986) (hereafter PE). The first one assumes an *unsteady* outflow. Rapid variations in the outflow’s Lorentz factor result in internal collisions, converting kinetic energy to synchrotron radiation of accelerated electrons. On the other hand, the ES scenario considers that the relativistic outflow is decelerated by an external circum-burst medium (hereafter CBM). Fi-

nally, PE models rely on efficient emission by the plasma, as it becomes optically thin when the plasma density and temperature drop due to the outflow’s expansion.

Several improvements were considered for each of these models in order to allow them to explain all bursts. However, it appears that they all have problems to explain certain specific features in specific bursts. Among them, GRB 090902B, with its nearly thermal spectrum, cannot be reconciled with either IS nor ES (Ryde et al. 2010), and the very smooth pulsed GRB 141025A which is well-explained by ES (Burgess et al. 2015).

Still, all three models have the potential to explain several features of GRBs. In fact, all three emission mechanisms are expected in *any* GRB scenario. Only their relative luminosities have to be quantified and the delay (for an observer) between them constrained. Sari (1997) considered the situation of an early onset of the afterglow (due to an external shock), which leads to mixed emission from an unspecified mechanism during the prompt phase of the GRB and the external shock. More recently, this idea was also put forth by Kumar & Barniol Duran (2009), who tried to explain the late onset of the GeV emission with synchrotron emission of electrons accelerated at the external shock.

In this paper, we consider the expansion of a classical thermal fireball (Goodman 1986; Paczyński 1986; Piran et al. 1993), for which magnetic fields are sub-dominants. There also exist magnetic acceleration models based on the spreading of magnetic lines, see *i.e.* Narayan et al. (2007) or magnetic reconnection (Drenkhahn & Spruit 2002; Giannios 2006). However, these models might be challenged by observations, see Bromberg et al. (2015); Bégué & Pe’er (2015). In addition, the classical thermal fireball model neglects the interaction between the progenitor of the GRBs, thought to be a massive star undergoing collapse (Woosley 1993; Woosley & Bloom 2006). However, numerical simulations have shown that, if the central engine remains active long enough, the expansion of the jet is mostly unperturbed once it has opened a funnel

¹ The Oskar Klein Centre for Cosmoparticle Physics, AlbaNova, SE-106 91 Stockholm, Sweden

² Department of Physics, KTH Royal Institute of Technology, AlbaNova University Center, SE-106 91 Stockholm, Sweden

[†] jamesb@kth.se

[‡] damienb@kth.se

⁵ The GRB emission is expected to be collimated in a narrow jet. However, in the following, we only deal with isotropic-equivalent quantities.

in the progenitor (Lazzati et al. 2012). Oblique shocks can also stall the initial expansion of the jets (Thompson et al. 1994; Iyyani et al. 2013), but here we neglect this effect.

In this paper, we propose to characterize the emission mechanisms solely based upon the dimensionless entropy of the outflow $\eta \equiv E_{\text{tot}}/(Mc^2) \gg 1$, where E_{tot} is the total energy of the burst, M is the total baryonic mass of the outflow, and c the speed of light.

First, we review all three models in their unembellished version and their main characteristics. Second, we come to the point of the paper and we show how the value of the dimensionless entropy strongly constrains all three emission mechanisms. Then, we analyse the implications and predictions of our classification on the afterglow and other GRB properties. Finally, we demonstrate how our classification can be tested against observations.

2. EMISSION MODELS

The ‘‘classical’’ fireball model (Paczynski 1990; Piran et al. 1993) assumes that a large quantity of energy $E_{\text{tot}} \sim 10^{53}$ erg is released by an unspecified cataclysmic event such as the death of a hyper-massive star. From the millisecond variability observed in a few GRBs (but not all, see Golkhou & Butler (2014)), the origin of the outflow is constrained to within a few 10^8 cm from the center of the progenitor. Such a large amount of energy in such a small region leads to the creation of an optically thick plasma. Due to its high thermal pressure, the outflow expands and is accelerated to relativistic speeds. The expansion can be described by two phases (Piran et al. 1993). During the initial accelerating phase, the Lorentz factor of the outflow increases proportionally to the radius, while after (eventually) reaching its limiting Lorentz factor $\Gamma \lesssim \eta$, the outflow coasts at constant velocity.

Other acceleration models based on magnetic fields are currently strongly debated in the literature (Drenkhahn & Spruit 2002; Narayan et al. 2007). However, our results can be re-parametrized to the magnetization of the outflow, which plays a comparable role to η for the expansion dynamics. Therefore, the results are expected to be *qualitatively* similar.

2.1. Photospheric model

In a photospheric model, the thermal energy is released when the outflow becomes transparent at typical radii $R_{\text{ph}} \sim 10^{10} - 10^{12}$ cm, for a recent review on photospheric emission, see Vereshchagin (2014). The efficiency of the photospheric emission, assuming no dissipation, can be evaluated as the ratio of the thermal energy emitted at the photosphere E_{th} to the total energy E_{tot}

$$\epsilon_{\text{ph}} = \frac{E_{\text{th}}}{E_{\text{tot}}} \sim 1 - \frac{\Gamma_{\text{ph}}}{\eta}, \quad (1)$$

where Γ_{ph} is the Lorentz factor at the photosphere. Therefore, a bright photosphere requires $\Gamma_{\text{ph}} \ll \eta$, implying transparency of the outflow in the initial accelerating phase or in the transition phase between accelerating and coasting phases. The limiting η value separating photospheric emission in the accelerating phase from transparency in the coasting phase is (Rees & Mészáros 1994; Thompson 1994)

$$\begin{aligned} \eta^* &= \left(\frac{\sigma_{\text{T}} E_{\text{tot}}}{4\pi m_{\text{p}} c^3 \Delta t R} \right)^{\frac{1}{4}} \\ &\sim 7 \times 10^2 E_{53}^{\frac{1}{4}} R_8^{-\frac{1}{4}} \Delta t_{5s}^{-\frac{1}{4}}, \end{aligned} \quad (2)$$

where R is the radius at which the outflow starts to accelerate, Δt is the time the central engine remains active, σ_{T} is the Thompson cross-section, m_{p} is the proton mass. For all parameters but Δt , which is normalized to 5s (see below), we adopt the convention $X = 10^n X_n$, where all quantities X are in CGS units. When $\eta > \eta^*$, more than half of the energy of the burst is emitted at the photosphere. Therefore, in this case, we consider that the emission from the photosphere dominates the emission of the prompt phase, regardless of which mechanism is responsible for any remaining emission. We further restrain the study to $\eta < \eta^*$ and consider the emission be dominated by photospheric emission for $\eta > \eta^*$.

In first approximation, as soon as the outflow becomes transparent, the radiative pressure decreases abruptly, stopping the acceleration of the outflow.⁶ This implies that the kinetic energy of the blast wave above the photosphere is set by Γ_{ph} . Neglecting high-latitude effects, the duration of the photospheric emission is roughly given by the light crossing time of the outflow $\Delta t_{\text{ph}} \sim \Delta t \sim l/c \sim$ few seconds, independent of the value of the Lorentz factor⁷. Here $l \sim c\Delta t$ is the laboratory width of the outflow. The luminosity at the photosphere is then approximated by:

$$L_{\text{ph}} = \epsilon_{\text{ph}} \frac{E_{\text{tot}}}{\Delta t}. \quad (3)$$

An important assumption in this derivation, is that, if dissipation occurs below the photosphere, it only amounts for a few percent of the total energy E_{tot} . This is in agreement with the analysis of spectra in the guise of a photospheric model, see *i.e.* Ahlgren et al. (2015). In addition, it was demonstrated in Bégué & Iyyani (2014) that if dissipation amounts for a large fraction of the total energy, the resulting observed photospheric peak energy would be too low (around 1keV) to corresponds to the peak energy of GRBs or to the additional blackbody component identified in some bursts (Ghirlanda et al. 2003; Ryde 2004).

2.2. Internal shock model

As the expanding outflow is unlikely to be steady due to small variations in the wind parameters, sections with different speeds will necessarily collide with one another. These collisions (internal shocks) convert a fraction of the kinetic energy to internal energy, which can subsequently be radiated away by accelerated electrons. The collided sections will then form a single merged system.

⁶ Here, we assume that the Compton drag is negligible, as implied by $\eta < \eta^*$, see equations (10) and (11) of Mészáros & Rees (2000). However, if $\eta \gg \eta^*$, then the flow is still accelerated above the photosphere. See a complete discussion in Grimsrud & Wasserman (1998) and Mészáros & Rees (2000). In the following we do not consider this effect, as we consider $\eta < \eta^*$.

⁷ This is true if high-latitude effects are neglected. They might be identified as the flux and temperature of the blackbody decreases as $F_{\text{BB}} \propto t^{-2}$ and $T_{\text{BB}} \propto t^{-2/3}$, see Pe'er (2008).

These collisions take place at typical radii⁸ $R_{\text{IS}} \sim 10^{14}$ cm. In this section, we follow the derivation of Daigne & Mochkovitch (1998) to obtain qualitative estimates. Assuming a steady injection mass rate and a Lorentz factor variation $\Delta\Gamma$, the Lorentz factor of the merged system after an internal shock Γ_{IS} is (Daigne & Mochkovitch 1998)

$$\Gamma_{\text{IS}} = \sqrt{\Gamma_{\text{ph}}(\Gamma_{\text{ph}} - \Delta\Gamma)} \sim \left(1 - \frac{\Delta\Gamma}{2\Gamma_{\text{ph}}} - \frac{\Delta\Gamma^2}{8\Gamma_{\text{ph}}^2}\right)\Gamma_{\text{ph}}, \quad (4)$$

where the last equality is obtained for $\Delta\Gamma < \Gamma_{\text{ph}}$.

The efficiency of this process can be estimated as (Kobayashi et al. 1997)

$$\begin{aligned} \epsilon_{\text{IS}} &= \frac{E_{\text{kin}} - E_{\text{kin,IS}}}{E_{\text{kin}}} = 1 - \frac{2\Gamma_{\text{ph}} \left(1 - \frac{\Delta\Gamma}{2\Gamma_{\text{ph}}} - \frac{\Delta\Gamma^2}{8\Gamma_{\text{ph}}^2}\right)}{(2\Gamma_{\text{ph}} - \Delta\Gamma)} \\ &\sim \frac{\Delta\Gamma^2}{8\Gamma_{\text{ph}}^2} \end{aligned} \quad (5)$$

Here $E_{\text{kin,IS}} = (1 - \epsilon_{\text{ph}} - \epsilon_{\text{IS}})E_{\text{tot}} = \epsilon E_{\text{tot}}$ is the kinetic energy of the outflow after dissipation of energy by IS. This hydrodynamical efficiency should be multiplied by an additional factor $\xi_{\text{rad,IS}} < 1$ to obtain the radiative efficiency. Then the luminosity of an IS is roughly given by:

$$L_{\text{IS}} = \xi_{\text{rad,IS}} \frac{\epsilon_{\text{IS}}(1 - \epsilon_{\text{ph}})E_{\text{tot}}}{\alpha_{\text{IS}}\Delta t}, \quad (6)$$

where $\alpha_{\text{IS}} > 1$ is a numerical factor of order unity, which takes into account that the IS duration for the observer is slightly larger than the light crossing time of the outflow, see Daigne & Mochkovitch (1998).

For efficient internal shocks, i.e., $\Delta\Gamma \simeq \Gamma_{\text{ph}}$, with high η , it is clear that the outflow must be very unsteady. Moreover, if the acceleration is incomplete at the photosphere ($\Gamma_{\text{ph}} \ll \eta$), the efficiency does not increase since $\Delta\Gamma$ and the Lorentz factor scale proportionally to the radius in the accelerating phase.

The strength of the model is its ability to reproduce the observed highly variable light curves of GRBs, down to the millisecond time-scale. However, the model has a low radiative efficiency on the order of a few percent (Kobayashi et al. 1997), implying that the emission can be out-shined by the photospheric emission (Daigne & Mochkovitch 2002), but also by an external shock, which will necessarily result as the outflow expands and interacts with the CBM.

2.3. External shock model

Initially proposed by Rees & Mészáros (1992), external shocks were studied in detail by Chiang & Dermer (1999) and Panaitescu & Mészáros (1998). As the relativistic blast wave expands, it substantially slows at the deceleration radius

⁸ One can imagine collisions at smaller radii even below the photosphere, see (Rees & Mészáros 2005). However, here we consider pure internal shocks as in their original definition.

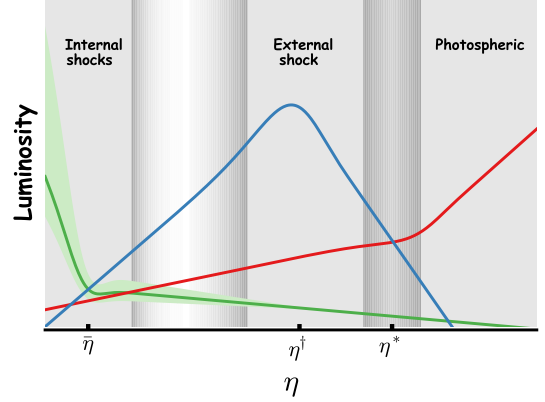


Figure 1. Cartoon showing the luminosity of the different emission mechanisms in function of the dimensionless entropy. At low η , the emission is dominated by internal shocks (in green). At intermediate values of the dimensionless entropy, external shock (in blue) becomes the dominant emission mechanism, while at large η the spectrum is expected to be nearly thermal, as mainly originating from the photosphere (in red).

$$\begin{aligned} R_{\text{ES}} &= \left(\frac{3E_{\text{kin,IS}}}{4\pi m_p c^2 n \Gamma_{\text{IS}}^2}\right)^{\frac{1}{3}} \\ &= 1.2 \times 10^{17} E_{\text{tot},53}^{\frac{1}{3}} n_0^{-\frac{1}{3}} \epsilon^{-\frac{1}{3}} \eta_2^{-\frac{2}{3}} \quad [\text{cm}] \end{aligned} \quad (7)$$

where n is the density of the interstellar medium. The last equality is obtained with $\Gamma_{\text{IS}} = \epsilon\eta$, implied by energy conservation. As the interaction between the outflow and the CBM develops, two shocks are created: the forward shock which expands into the CBM, and the reverse shock which collides back into the outflow. If the reverse shock is not relativistic, the emission peak time is (Sari 1997)

$$t_{\text{ES}} = \frac{R_{\text{ES}}}{\Gamma_{\text{IS}}^2 c} = \left(\frac{3}{4\pi m_p c^5 n}\right)^{\frac{1}{3}} \left[\frac{E_{\text{tot}}}{\epsilon^6 \eta^8}\right]^{\frac{1}{3}} \quad (8)$$

which is strongly dependent on η . This time-scale also corresponds to the time delay between the beginning of the photosphere-IS emissions and the peak of the ES emission⁹.

In addition, the luminosity of the forward shock before t_{ES} can be expressed as (Sari 1997)

$$L_{\text{ES}} = \xi_{\text{rad,ES}} 32\pi c^5 n m_p \Gamma_{\text{IS}}^8 t^2, \quad (9)$$

where t is the observed time after trigger and $\xi_{\text{rad,ES}}$ is the radiative efficiency of the external shock.

2.4. Thin or thick outflow?

The typical prompt phase duration of a long GRBs T_{dur} is on average a few tens of seconds. In the IS and PE framework, this duration is tightly associated to the light-crossing time of the outflow (Daigne & Mochkovitch 1998; Pe'er 2015)

⁹ The delay between IS and PE photons is small compared to the long bursts duration and is neglected hereafter.

$$T_{\text{dur}} = \alpha \frac{l}{c} = \alpha \Delta t. \quad (10)$$

Because of redshift dilation, we normalise our computation to $\Delta t = 5\text{s}^{10}$, keeping in mind that it might be much larger.

By requiring t_{ES} to be smaller than $\Delta t/2$ such that photons from the prompt phase originate from all three mechanisms combined (PE, IS and ES), it follows that:

$$\eta > \eta^\dagger = \left(\frac{6E_{\text{tot}}}{\pi n m_p c^5 \Delta t^3 \epsilon^7} \right)^{\frac{1}{8}} \quad (11)$$

$$\sim 6.6 \times 10^2 \epsilon^{-\frac{7}{8}} E_{53}^{\frac{1}{8}} n_0^{-\frac{1}{8}} \Delta t_{5s}^{-\frac{3}{8}}. \quad (12)$$

Comparing η^\dagger to η^* gives a minimum energy for the burst such that the photosphere does not take place in the accelerating phase and the external shock peaks in the prompt phase:

$$E_{\text{tot}} > E_* = 6.9 \times 10^{52} R_g^2 \Delta t_{5s}^2 \epsilon^{-7} \quad [\text{erg}]. \quad (13)$$

The strong dependence on the parameters has to be noted. Therefore, we conclude that only very energetic bursts of total energy $E_{\text{tot}} > \text{few } 10^{53}$ ergs can have a simultaneous emission from all three mechanisms.

It can be shown that requiring $\eta \gg \eta^\dagger$ implies that the reverse shock is relativistic (Sari 1997). However, here we use t_{ES} as a proxy for the peak emission time of the ES. For instance, density gradients in the ISM below R_{ES} result in variability of the ES emission before t_{ES} , which might also outshine the IS emission.

3. DOMINANT EMISSION MECHANISM FOR A GRB

We now qualitatively analyse the requirements for each emission mechanism to be the dominant process during the prompt phase of GRBs.

3.1. Case 1: IS dominates the prompt emission

In a situation in which the main component of the prompt emission is due to internal shocks, because of the low efficiency of an internal shock, three conditions should be met:

1. the photospheric emission should be dim, that is to say that $\Gamma_{\text{ph}} \simeq \eta$. From the theory of the photospheric emission (see *e.g.* Vereshchagin (2014) for a review) it comes that lower η implies a smaller difference between the Lorentz factor at the photosphere and the dimensionless entropy, and also a lower brightness of the photosphere.
2. the onset of the ES should take place at late times and it should be dim. From Equations (8) and (9), it follows that η has to be small.

Therefore, combining the first and last points implies that η cannot be too large. If this condition is violated,

¹⁰ Actually, Gruber et al. (2011) showed that the typical rest-frame duration of *Fermi* bursts is around 12s. Even if normalised to 5s, we find that the following results are weakly dependent on the duration Δt .

the IS emission would be out-shined by the photospheric and/or the ES emission. To estimate the value of η such that the luminosity of the internal shock is larger than that of the ES at the peak, we combine Equations (6), (8) and (9):

$$\begin{aligned} \eta < \bar{\eta} &= \frac{1}{\epsilon^{\frac{3}{2}}} \left(\frac{1}{8 * 3^{\frac{2}{3}}} \frac{\xi_{\text{rad,IS}}}{\xi_{\text{rad,ES}}} \frac{\epsilon_{\text{IS}}}{\alpha \Delta t} \right)^{\frac{3}{8}} \left(\frac{E_{\text{tot}}}{4\pi m_p c^5 n} \right)^{\frac{1}{8}} \\ &= 1.1 \times 10^2 \frac{E_{53}^{\frac{1}{8}}}{\Delta t_{5s}^{\frac{3}{8}} n_0^{\frac{1}{8}}}, \end{aligned} \quad (14)$$

weakly dependent on the total energy of the burst or on the CBM density. For the numerical estimate, we choose $\alpha = 1$ and $\epsilon = 1 - \epsilon_{\text{IS}} = 0.8$ (with such a small Lorentz factor, the photospheric emission is expected to be very dim $\epsilon_{\text{ph}} \ll \epsilon_{\text{IS}}, \epsilon_{\text{ES}}$). In addition, the radiative efficiency of the IS and ES are set equal: $\xi_{\text{rad,ES}} = \xi_{\text{rad,IS}}$.

Therefore, an ES should easily outshine the emission from IS. However, with such a low Lorentz factor ($\bar{\eta} < \eta^\dagger$), the ES emission takes place at later times, leading to a burst composed of two episodes: a precursor followed by one or several smooth pulses from the external shock at later time.

3.2. Case 2: ES dominates the prompt emission

Let us now consider a situation in which the emission from the external shock dominates the prompt phase, which is only possible if $E_{\text{tot}} > E_*$, see Equation (13). For example, the prompt phase of GRB 141025A can be interpreted in the ES framework (Burgess et al. 2015). The requirements are:

1. the onset of the ES emission should be early. From Equation (8), one sees that it implies large η .
2. finally, the photospheric emission should not be too bright, which implies that the transparency is reached in the coasting phase, or in the late transition phase, implying $\Gamma_{\text{ph}} \lesssim \eta$.

Therefore, it follows that η should be large enough to produce the early onset of the afterglow, but small enough such that the transparency takes place in the coasting phase to avoid too bright of a photospheric emission $\eta < \eta^*$.

Here, we only considered a circum-burst medium with constant density. If the density has some variations below R_{ES} , a multi-peak light-curve with *second*-like variability is formed.

3.3. Case 3: PE the prompt emission

Finally, if the PE dominates the prompt emission like for GRB 090902B¹¹ (Ryde et al. 2010), several constraints can also be obtained

1. a bright photosphere requires the transparency to take place in the accelerating phase or in the transition regime, implying large η and $\Gamma_{\text{ph}} \ll \eta$, that is to say $\eta \sim \eta^*$

¹¹ Even if this burst is very unique, it perfectly fits in the classification scheme.

Table 1
Spectral and temporal characteristics and/or predictions of GRBs dominated by each three emission mechanisms.

		Internal Shocks	External Shocks	Photospheric emission
Temporal Properties	Variability	Highly variable	Smooth pulse	Medium to high variability
	Peaks	Several	One / several very smooth	Several
	Afterglow	Weak and late onset	Continuous decay	Weak and early onset
	Afterglow decay index	Can be steep $\delta > 3$	$\delta \sim 1.2$	Can be steep $\delta > 3$
Spectral properties	Thermal component	Weak to bright for low E_{tot}	Weak	Dominant
	Temporal correlations	Yes	No	No
	Low energy spectral index	$> -2/3^{\text{a}}$	Soft $\alpha \sim -0.67$	Hard $\alpha \sim 0$
	Pair cut-off	~ 100 MeV	~ 1 GeV	-
Other	Efficiency	Low	Middle to high	High

^aThis is for synchrotron emission, discarding possible Klein-Nishina effects (Daigne et al. 2011).

2. Finally, a late onset of the ES is required and is obtained for low Γ_{ph} , as implied by the requirement $\eta > \eta^*$.

Therefore, a dominant photosphere requires an incomplete acceleration.

To conclude, we have shown here that for IS to be the dominant process, low η and the transparency in the deep coasting phase are required. For ES, an intermediate value of η with the transparency reached in the coasting phase are required. Finally, a spectrum dominated by photospheric emission is obtained if transparency is reached in the accelerating phase, requiring large $\eta \gtrsim \eta^*$. We note that such results for PE and ES only were already obtained by Muccino et al. (2013), who considered the photospheric emission as a precursor of the main burst explained by an ES. This is illustrated by a cartoon in Figure 1.

4. ADDITIONAL OBSERVATIONAL CONSTRAINTS

The classification scheme proposed here imposes several observational predictions and requirements, which are summarised by Table 1. Here we discuss in turn the temporal and spectral properties of GRBs dominated by one of the three mechanisms.

Both the PE and IS models can produce highly variable¹² and complex (multiples peaks with no correlations between time and the amplitude/width of a peak) light-curves. However, the ES model cannot easily explain variability below the second time-scale without fine tuning. In addition, the ES model can produce several peaks by adding density variations in the ISM. However, the duration of each episode should increase and the luminosity decay should become shallower. GRB 090618 is an example of such kind of bursts (Zhang 2012): after a first episode lasting around 50s, which might be associated to PE and/or IS, there are three episodes with increasing width and decreasing maximum luminosity, which can be interpreted in the ES framework.

¹² The IS model was initially proposed to explain sharp flux decreases on the millisecond time-scale. Such variability is hardly achieved by PE models without fine tuning of the plasma emission at the central engine, and a more realistic variability time-scale might be 0.1-1s.

The link between the prompt phase and the “afterglow” also sets tight constraints. Indeed a break in luminosity at the very end of the prompt phase observed by *Swift* cannot easily be explained by an ES, for which a shallow decay is expected (see however Dermer 2007, who proposed that the decay be explained by a strongly radiative phase triggered by a hadronic discharge). The steep decay might however be characteristic of an efficient PE or IS model and a low Lorentz factor for the blast wave after transparency and dissipation by IS, such that the ES emission is delayed to late times and its luminosity decreased.

The energy requirement to have the ES occurring simultaneously with PE or IS given by Equation (13) implies that a shallow decay of the afterglow, if due to an external shock, is correlated to large total energy $E_{\text{tot}} \gg E_*$. This can easily be checked in the data and is currently under investigation.

Finally, the large difference between η^* and $\bar{\eta}$ implies that numerous bursts should have (at least) two time-separated components in their light-curve: first the emission from the photosphere and the IS, followed by the emission of the ES.

Several constraints can also be obtained from the spectral shape of a burst. First the relative luminosity of the thermal component and the time evolution of its flux and temperature, as compared to that of the non-thermal emission can give clues to identifying the emission mechanism. In particular, in an IS-PE model, the blackbody properties are likely to track the non-thermal flux evolution, while it should not be the case in a ES-PE model.

The rather low Lorentz factor implied if the emission originates from an IS suggests that a cut-off be present in the spectra at moderate energy of around hundreds of MeV, see Hascoët et al. (2012), while larger Lorentz factor as achieved for a dominant photosphere or ES increases the cut-off to larger energy. The presence or absence of this cut-off can be investigated with the *Fermi-LAT* instrument.

Finally, the modelling of the afterglow can help to constrain the efficiency of the prompt emission. Together with its spectral characteristics (specifically the identification of a blackbody), the emission mechanism might be

constrained as low efficiency is expected from IS, medium from ES and high from PE.

Above, we only mentioned pure cases. However, hybrid bursts are expected to be numerous. As an example of hybrid, several bursts with envelopes (Vetere et al. 2006) might be explained by two of the aforementioned emission mechanisms. The univocal determination relies on a detailed spectral analysis of each component separately.

5. DISCUSSION

The approach followed in this letter to determine the efficiency of each emission mechanism is simple, and more detailed computations can be done. As an example, the ES luminosity and peak energy are usually determined in the literature by introducing two additional parameters ϵ_B and ϵ_e , which parametrize the microphysics (magnetic content and internal energy in random motion of electrons) of the shocked plasma. Precise values of these parameters are unknown, and limits are often obtained such that the emission of the forward shock is not detectable in the MeV band (Kumar & Barniol Duran 2009), which usually translates to low density n_0 and low ϵ_B . However, we note that the limits on the Lorentz factor do not change substantially with the introduction of ϵ_B and ϵ_e , which justifies our simplified treatment.

Furthermore, our analysis of the photospheric emission is based on the identification of a black-body. This might be hampered by sub-photospheric dissipation, *i.e.* below the photosphere, which could result in strong distortion of the emerging spectrum. Examples of dissipation mechanisms are neutron decay (Beloborodov 2010), internal shocks (Rees & Mészáros 2005) or dissipation of magnetic energy (Giannios 2006).

Finally, we did not consider outflows where acceleration is powered by magnetic fields. On one hand, such outflows are challenged by observations (Bégué & Pe'er 2015; Bromberg et al. 2015). On the other hand, it might be possible that some GRBs outflows be powered by magnetic fields. Theoretically, the dynamics is parametrized by the magnetisation $\sigma = E_{\text{mag}}/Mc^2$, where E_{mag} is the initial energy in magnetic fields. As for thermally powered outflows, σ plays the same role as η . In particular, it scales the coasting Lorentz factor of the outflow. The determination of spectral and/or temporal criteria to distinguish between thermal and magnetic acceleration is the next step towards a more detailed classification of emission mechanisms of GRBs, but it is out of the scope of this paper. We also note that if the outflow is strongly magnetized, IS are very inefficient. However, the magnetic field can be dissipated at larger radii by magnetic reconnection, accelerating electrons which radiate synchrotron, see the ICMART model (Zhang & Yan 2011).

To conclude, we have studied the possibility that the three main emission mechanisms (PE, IS, ES) discussed in the literature be reliable mechanisms to explain the prompt phase of GRBs. We found that the dimensionless entropy and the corresponding Lorentz factors scales the relative luminosity of each mechanisms. The delay between each emission is also strongly increased with small Lorentz factors, which implies that bursts with several episodes (in the MeV energy band) exists. This work presents a simple attempt in classifying the emission mechanisms of GRBs.

The authors are thankful to Peter Mészáros, Asaf

Pe'er, Tsvi Piran and Felix Ryde for discussions which helped improving the manuscript.

DB is supported by a grant from Stiftelsen Olle Engkvist Byggmästare.

REFERENCES

- Abbasi, R., Abdou, Y., Abu-Zayyad, T., et al. 2012, *Nature*, 484, 351
- Ahlgren, B. and Larsson, J. and Nymark, T. and Ryde, F. and Pe'er, A. 2015, *MNRAS*, 454, 31
- Bégué, D., & Pe'er, A. 2015, *ApJ*, 802, 134
- Bégué, D., & Iyyani, S. 2014, *ApJ*, 792, 42
- Beloborodov, A. M. 2010, *MNRAS*, 407, 1033
- Bromberg, O., Granot, J., & Piran, T. 2015, *MNRAS*, 450, 1077
- Burgess, J. M., Bégué, D., Ryde, F., et al. 2015, *ArXiv e-prints*, arXiv:1506.05131
- Chiang, J., & Dermer, C. D. 1999, *ApJ*, 512, 699
- Daigne, F., Bošnjak, v., & Dubus, G. 2011, *A&A*, 526, A110
- Daigne, F., & Mochkovitch, R. 1998, *MNRAS*, 296, 275
- . 2002, *MNRAS*, 336, 1271
- Dermer, C. D. 2007, *ApJ*, 664, 384
- Drenkhahn, G., & Spruit, H. C. 2002, *A&A*, 391, 1141
- Ghirlanda, G. and Celotti, A. and Ghisellini, G. 2003, *A&A*, 406, 879
- Giannios, D. 2006, *A&A*, 457, 763
- Golkhou, V. Z., & Butler, N. R. 2014, *ApJ*, 787, 90
- Goodman, J. 1986, *ApJ*, 308, L47
- Grimsrud, O. M., & Wasserman, I. 1998, *MNRAS*, 300, 1158
- Gruber, D., Greiner, J., von Kienlin, A., et al. 2011, *A&A*, 531, A20
- Hascœt, R., Daigne, F., Mochkovitch, R., & Vennin, V. 2012, *MNRAS*, 421, 525
- Iyyani, S., Ryde, F., Axelsson, M., et al. 2013, *MNRAS*, 433, 2739
- Kobayashi, S., Piran, T., & Sari, R. 1997, *ApJ*, 490, 92
- Kumar, P., & Barniol Duran, R. 2009, *MNRAS*, 400, L75
- Kumar, P., & Zhang, B. 2015, *Phys. Rep.*, 561, 1
- Lazzati, D. and Morsony, B. J. and Blackwell, C. H. and Begelman, M. C. 2012, *ApJ*, 750, 68
- Mészáros, P. 2006, *Reports on Progress in Physics*, 69, 2259
- Mészáros, P., & Rees, M. J. 1993, *ApJ*, 405, 278
- . 2000, *ApJ*, 530, 292
- Muccino, M., Ruffini, R., Bianco, C. L., Izzo, L., & Penacchioni, A. V. 2013, *ApJ*, 763, 125
- Narayan, R., McKinney, J. C., & Farmer, A. J. 2007, *MNRAS*, 375, 548
- Paczynski, B. 1986, *ApJ*, 308, L43
- . 1990, *ApJ*, 363, 218
- Panaiteanu, A., & Mészáros, P. 1998, *ApJ*, 492, 683
- Pe'er, A. 2008, *ApJ*, 682, 463
- Pe'er, A. 2015, *Advances in Astronomy*, 2015, 907321
- Piran, T., & Shemi, A. 1993, *ApJ*, 403, L67
- Piran, T., Shemi, A., & Narayan, R. 1993, *MNRAS*, 263, 861
- Rees, M. J., & Mészáros, P. 1992, *MNRAS*, 258, 41P
- . 1994, *ApJ*, 430, L93
- . 2005, *ApJ*, 628, 847
- Ryde, F. 2004, *ApJ*, 614, 827
- Ryde, F., Axelsson, M., Zhang, B. B., et al. 2010, *ApJ*, 709, L172
- Rykoff, E. S., Aharonian, F., Akerlof, C. W., et al. 2009, *ApJ*, 702, 489
- Sari, R. 1997, *ApJ*, 489, L37
- Thompson, C. 1994, *MNRAS*, 270, 480
- Thompson, C. and Mészáros, P. and Rees, M. J. 2007, *ApJ*, 666, 1012
- Vereshchagin, G. V. 2014, *International Journal of Modern Physics D*, 23, 30003
- Vetere, L., Massaro, E., Costa, E., Soffitta, P., & Ventura, G. 2006, *A&A*, 447, 499
- Woosley, S. E. 1993, *ApJ*, 405, 273
- Woosley, S. E., & Bloom, J. S. 2006, *ARA&A*, 44, 507
- Zhang, B., & Yan, H. 2011, *ApJ*, 726, 90
- Zhang, F.-W. 2012, *Ap&SS*, 339, 123